



GO@dopamine-Cu as a Green Nanocatalyst for the Efficient Synthesis of Fully Substituted Dihydrofuran-2(5H)-ones

Neda Niknam¹ , Nader Noroozi Pesyan*¹ 

¹Department of Organic Chemistry, Faculty of Chemistry, Urmia University, 57159, Urmia, Iran

Abstract: A new nanocatalyst graphene oxide@dopamine-Cu was synthesized, and its structure was characterized by fourier transform infrared (FT-IR), X-ray diffraction (XRD), scanning electron microscopy (SEM), transmission electron microscopy (TEM), Energy Dispersive X-ray Spectrometry (EDX), and thermogravimetric analysis – differential thermal analysis (TGA-DTA) techniques. The three-component one-pot reaction between an arylamine, aromatic aldehyde, and acetylenic carboxylate was achieved and formed methyl 5-oxo-2-aryl-4-(arylamino)-2,5-dihydrofuran-3-carboxylate derivatives (**4**) in the presence of the catalytic amount of graphene oxide@dopamine-Cu nanocatalyst in high yield. Molecular structures of products were characterized by FT-IR, ¹H, ¹³C nuclear magnetic resonance (NMR), and Mass spectroscopy techniques. Representatively, the mass fragmentation of **4a** was discussed, and the structure was confirmed. Easy reaction, high performance, and easy catalyst recyclability are the main advantages of this work. This nanocatalyst is recycled up to five successive runs.

Keywords: Dihydrofuran-2(5H)-one, Dimethyl acetylenedicarboxylate, Green synthesis, Graphene oxide, Dopamine, Copper

Submitted: March 12, 2023. **Accepted:** November 24, 2023.

Cite this: Niknam N, Pesyan NN. GO@dopamine-Cu as a Green Nanocatalyst for the Efficient Synthesis of Fully Substituted Dihydrofuran-2(5H)-ones. JOTCSA. 2024; 11(1): 233-44.

DOI: <https://doi.org/10.18596/jotcsa.1264129>.

***Corresponding author. E-mails:** nnp403@gmail.com, n.noroozi@urmia.ac.ir.

1. INTRODUCTION

Nowadays, green chemistry and its features have caused nanocatalysts to be significant in organic synthesis and the development of green chemistry. In addition, much attention has been focused on preparing novel catalysts, which are important objects (1–3). Preparing new composites using graphene oxide (GO) has recently attracted much attention worldwide. In this regard, the GO supports many catalysts designation and is highly applicable. Some of the advantages of GO include its active sites and pores' thermal stability, high selectivity, and high mechanical strength (4,5).

Furthermore, there are various functional groups such as carbonyl, hydroxyl, carboxylic acid, and epoxide on GO sheets, in which GO can easily make covalent bonds to various functional groups in other

molecules. Also, the immobilization of some metallic nanoparticles (NPs) on GO made them used in many applications, such as catalysts, optoelectronics, and sensors for energy storage and generation (6–10). Using graphite oxidation for the synthesis of GO is one of the most known and useful protocols in the preparation of materials based on GO (11,12). Several oxygenic functional groups on GO sheet surface are caused to be hydrophilic (13), which can be reacted and functionalized by different reactants and organic ligands (14).

In recent years, multicomponent reactions (MCRs) have been one of the best tools in organic synthesis (15–19). The MCRs are one of the best ways to synthesize useful and accessible compounds used to synthesize pharmaceutical and drug compounds. The MCRs have a wide range of benefits such as high atom economy by reacting three or more

reactants in one step and the ability to synthesize assigned and desired compounds.

Many biologically active natural products and synthetic pharmaceutical drugs such as rubrolide A and benfurodil hemisuccinate have dihydrofuranone ring structure skeleton. The furanone five-membered heterocyclic compounds, including lactones, show a wide spectrum of biological and pharmacological behaviors such as anticancer, antibacterial, antifungal, and anti-oxidant (20–24). Full substituted furans are important in organic synthesis; they are important in many natural product compounds and are common structural textures in pharmaceuticals and flavors (25,26). Furan and dihydrofuran skeletons display several biological and pharmaceutical behaviors such as anticancer (27,28), anti-inflammatory (29,30), antimicrobial, (31–34) antifungal (35) and anti-viral HIV-1 (36) activities.

Several catalytic routes for the synthesis of 2(5*H*)-furanone were reported in the literature, e.g., acidic ionic liquid on silica-coated magnetic nanoparticles (19), graphene-oxide/Schiff base N₂O₄ ligand-palladium (14) and using BF@ Propyl /dopamine/ Palladium (37). Some synthetic routes have also been reported to access fully substituted furan derivatives, for example, the reaction of α -substituted ketones with β -dicarbonyl derivatives (38). Due to the eligibility and usability of these compounds, several various methods were achieved and used, such as Pd(Ph₃P)₂Cl₂ (34), Al(HSO₄)₃ (36), FeCl₃ (39), and lactic acid (40). These conditions suffer from the following problems, e.g., long reaction time, troublesome work-up, low yields, environmental pollution, and disagreeable reaction conditions. Herein, GO@dopamine-Cu as a recoverable nanocatalyst was used for the one-pot synthesis of full substituted dihydrofuran-2(5*H*)-one derivative (**4**) in high yield.

2. EXPERIMENTAL SECTION

2.1 Materials and Instruments

Chemicals were purchased from Fluka, Merck, and Aldrich Chemicals. All products were determined by comparing spectral data (¹H NMR and ¹³C NMR) and physical data with valid samples. FT-IR spectra were measured by a Perkin Elmer Spectrum Version 10.02.00 spectrometer using KBr pellets. Mass spectra were measured by a Shimadzu GC MS-QP 1000 EX. The Buchi 510 apparatus was used to obtain melting points. The ultrasonic apparatus for sonication was used SONICA 50Hz 230/240 V. The TEM, SEM, and EDX analyses were taken by Zeiss-EM10C-100KV, EM3200, and FESEM-SIGM (Germany), respectively. TGA analysis was measured using the PYRIS DIAMOND model.

2.2. Synthesis of GO@dopamine-Cu

2.2.1. Preparation of graphene oxide

In a 500-mL round bottom flask equipped with a magnetic stirrer, 2.5 g of natural graphite were placed together with 50 mL of concentrated sulfuric acid (98%). The mixture was swirled for 30 min. Subsequently, 1.25 g of sodium nitrate were added to the flask and violently mixed. Next, the reaction mixture was transferred from the flask into an ice bath. Proceed by introducing 7 g of potassium permanganate (KMnO₄) and gradually adding 25 mL of hydrogen peroxide (30% concentration) while continuously stirring the solution for 45 min. The reaction mixture, which was black, underwent a washing process using 1 mL of hydrochloric acid (37%). Subsequently, the mixture was subjected to centrifugation and subsequent drying.

2.2.2. Immobilization of 2-(3,4-dihydroxy phenyl)ethyl amine (dopamine) on graphene oxide

In a 250 mL round-bottom flask containing a magnetically stirred setup, 0.5 g of graphene oxide (GO) and 25 mL of toluene were combined and dispersed. The resulting mixture was subjected to sonication for 20 minutes at room temperature. Subsequently, a quantity of 1.5 g of dopamine was introduced and subjected to reflux for 24 hours. The precipitate was separated using filtration, followed by rinsing with a small amount of toluene and subsequently with ethanol. Finally, the precipitate was dried at 100 °C under vacuum conditions.

2.2.3. Synthesis of GO@dopamine/Cu

In a 50 mL round bottom flask equipped with a magnetic stirrer, put 0.5 gr GO@dopamine and the solution of 0.5 g (1 mmol) copper acetate in 10 mL acetonitrile. The reaction mixture was sonicated for 15 minutes and then stirred for 24 hrs at 90 °C. Afterwards, it was filtered off, washed with a few mL of acetone, and dried in an oven for 18 hrs at 50 °C.

2.3. General Procedure for the Synthesis of **4a** in the Presence of GO@dopamine/Cu as a Model Reaction

Dimethyl acetylenedicarboxylate (1 mmol), benzaldehyde (1 mmol), and aniline (1 mmol) were introduced into a 25 mL round bottom flask fitted with a magnetic stirrer. Additionally, 0.05 g of nanocatalyst was included in 15 mL of ethanol. The resulting mixture was subjected to stirring and refluxing for 30 minutes. The course of the reaction was seen through thin-layer chromatography (TLC) with a solvent mixture consisting of n-hexane and ethyl acetate at a ratio of 2:10 (v/v). Following the conclusion of the reaction, the resulting mixture was subjected to filtration, followed by a thorough washing with a small volume of ethanol. Subsequently, the obtained solid was subjected to recrystallization in hot ethanol. The spectral data for **4a** is shown here in a representative manner.

2.3.1. Methyl 5-oxo-2-phenyl-4-(phenylamino)-2,5-dihydrofuran-3-carboxylate (**4a**)

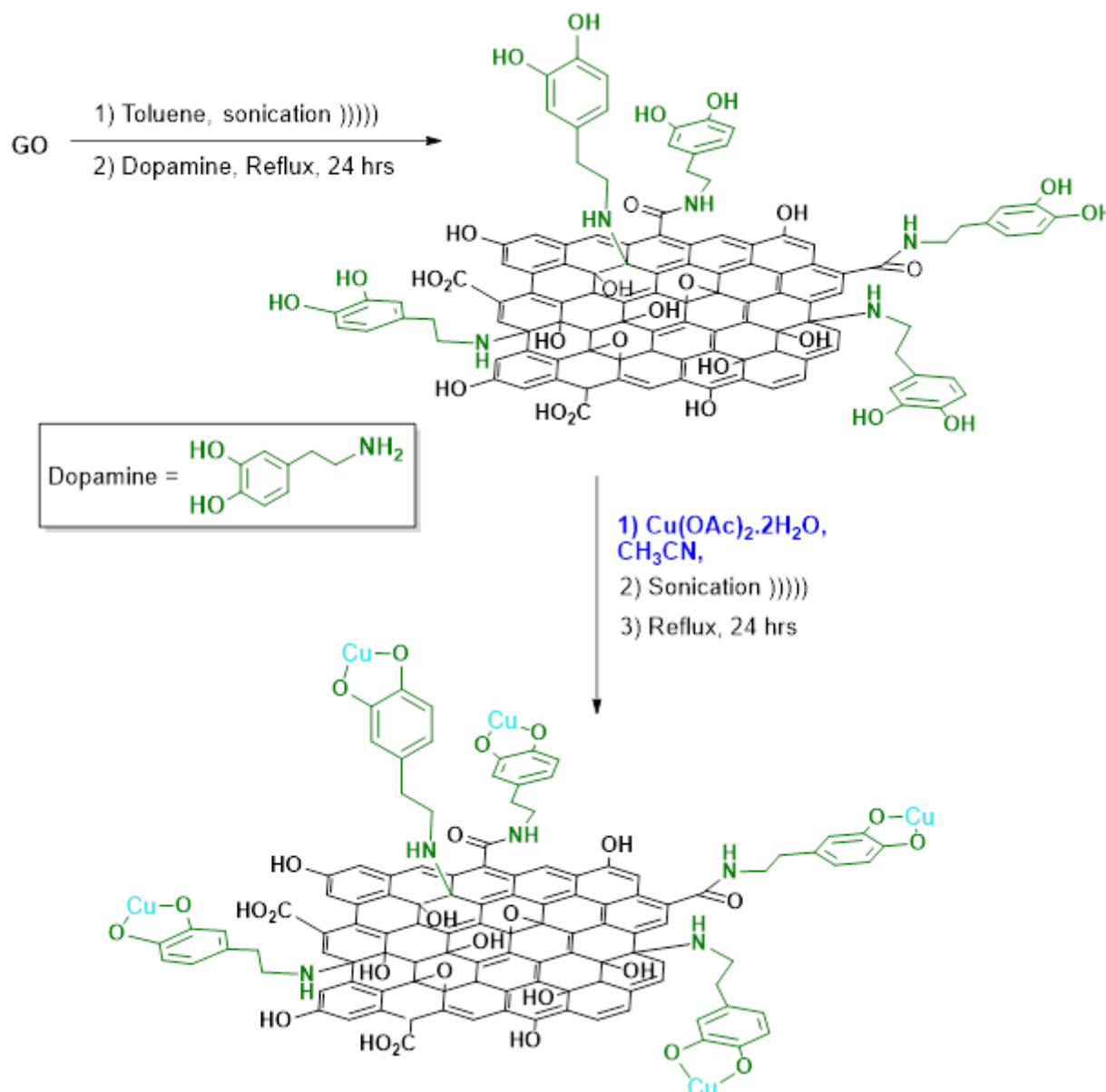
Light yellow solid (Yield: 85%); M.p. 187-189 °C; FT-IR (KBr): $\bar{\nu}$ (cm^{-1}) 3263, 3210, 2958, 1703, 1682, 1499, 1457, 1383, 1234, 1136, 755; ^1H NMR (400 MHz, $\text{DMSO-}d_6$, δ , ppm): 3.57 (s, 3H, OCH_3), 6.06 (s, 1H, CH), 7.07 (m, 1H, Ar-H), 7.24 (m, 7H, Ar-H), 7.55 (m, 2H, Ar-H), 11.74 (s, 1H, NH); ^{13}C NMR (100 MHz, $\text{DMSO-}d_6$, δ , ppm): 51.1, 60.5, 111.9, 122.5, 127.6, 128.2, 128.6, 136.2, 136.5, 152.5, 162.4, 163.9; MS (m/z): 309.1 (M^+ , 100%,

base peak), 277, 250, 222, 189, 158, 130, 102, 77, 51.

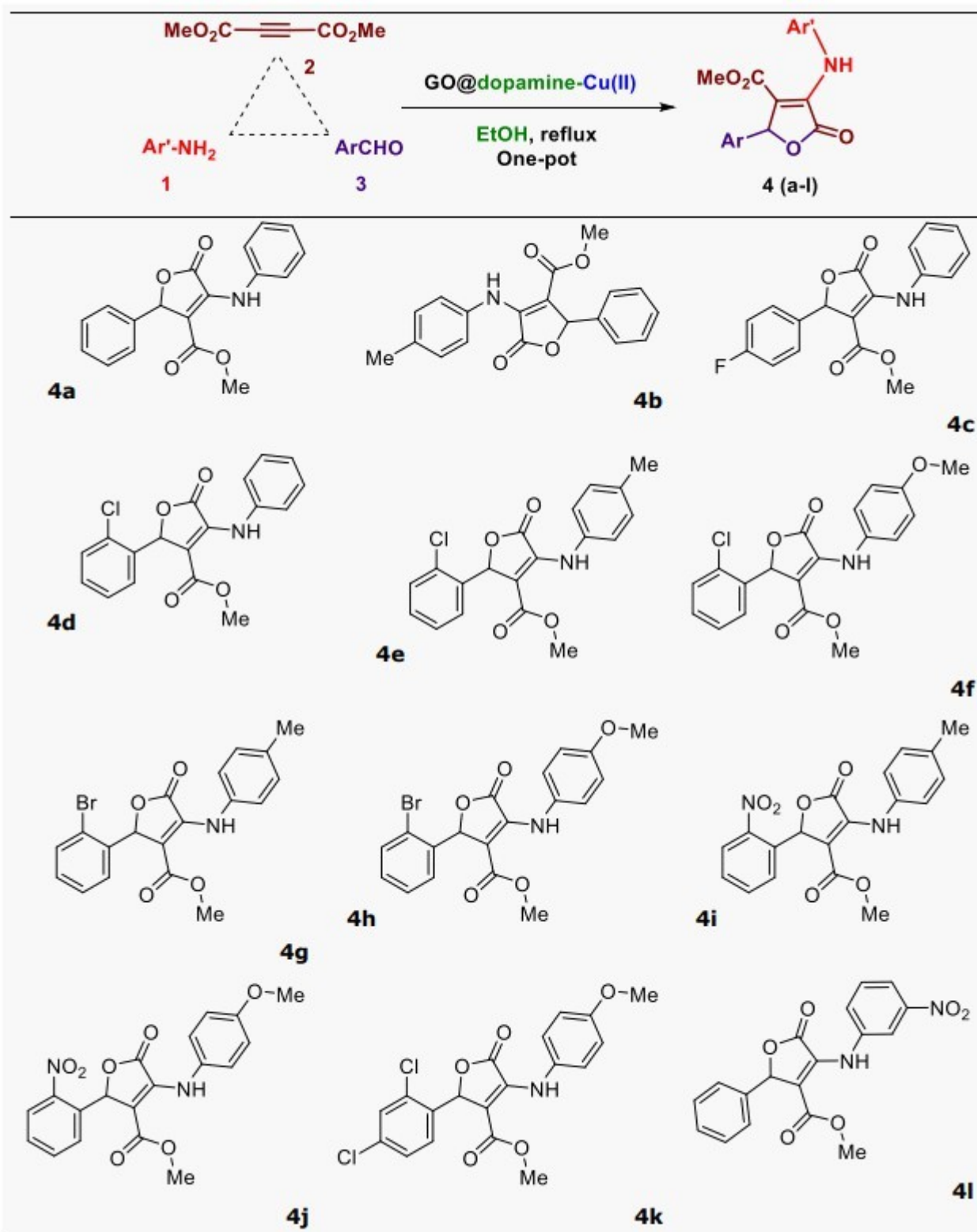
3. RESULTS AND DISCUSSION

3.1. Synthesis of Nanocatalyst and Dihydrofuran-2(5H)-one derivatives

This article first described the synthesis and characterization of a new nanocatalyst of GO@dopamine-Cu (Scheme 1) and followed using this nanocatalyst for the synthesis of dihydrofuran-2(5H)-one derivatives **4a-4l** (Table 1).



Scheme 1. Synthesis of GO@dopamine-Cu nanocatalyst.

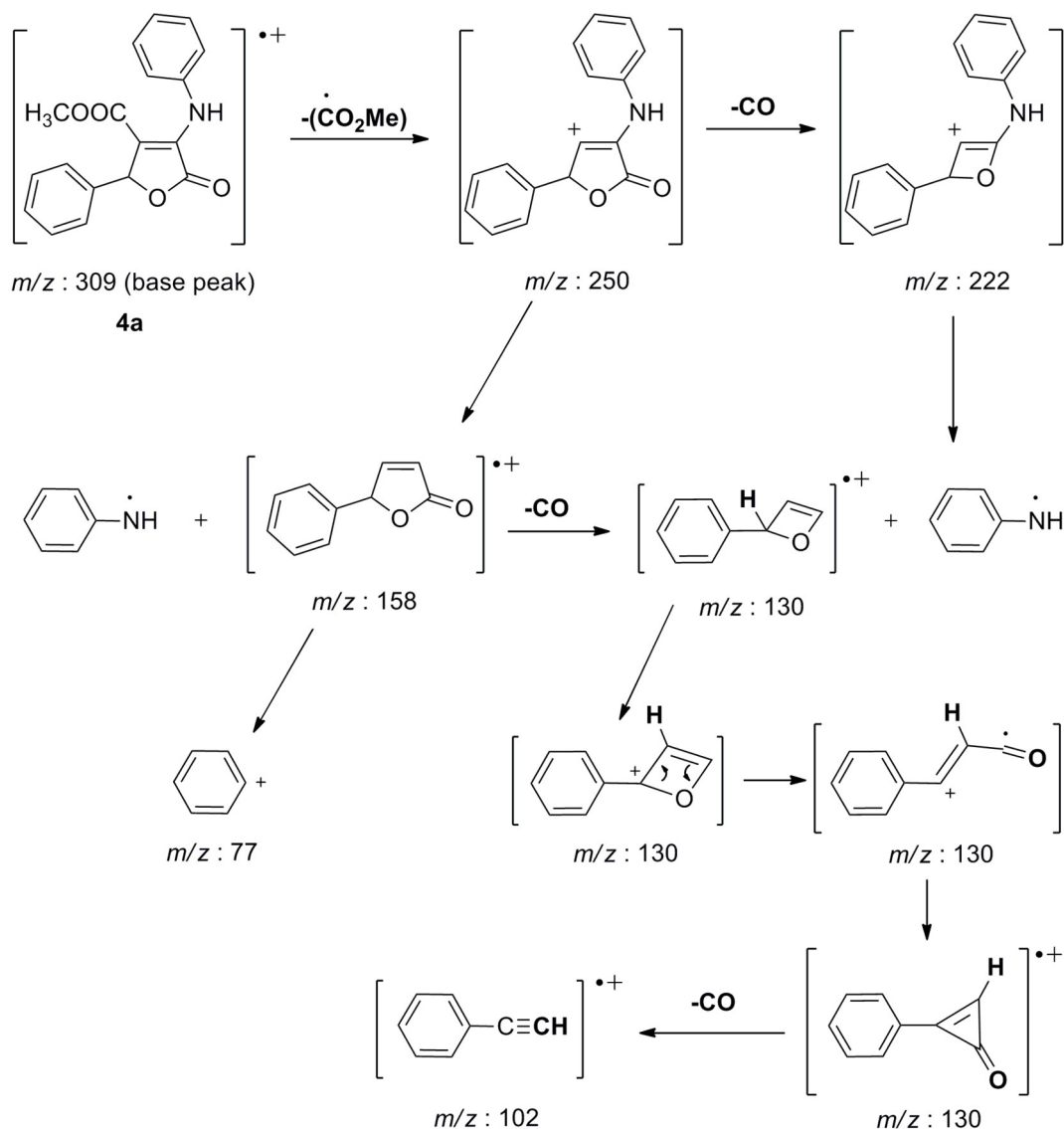
Table 1. Synthesis of dihydrofuran-2(5*H*)-one derivatives in the presence of GO@dopamine-Cu nanocatalyst.

Representatively, the FT-IR spectrum of **4a** showed two bands at 3262 and 3210 cm^{-1} for NH stretching frequencies. Two bands at 1702 and 1681 cm^{-1} correspond to two carbonyl stretching frequencies of dihydrofuran and methyl carboxylate carbonyl

groups, respectively. ^1H NMR spectrum of this compound showed a broad peak at δ 11.73 ppm for NH proton, at δ 7.10-7.54 ppm for two phenyl protons, a singlet at δ 6.53 ppm for benzylic CH proton, and finally, a singlet at δ 3.57 ppm for OMe

protons. ^{13}C NMR spectrum of this compound showed fourteen distinct peaks and confirmed the assigned structure. Representatively, the spectral data for **4a** is presented in the experimental section. (Other spectral data are available; for more information, see Supplemental materials). The MS

spectrum of **4a** showed m/z 309 (100%, base peak, molecular ion mass) as a molecular ion mass and a fragment at m/z 250 (75%) via the loss of methyl carboxylate fragment. The proposed full fragmentation of **4a** is shown in Scheme 2, confirming the assigned structure.



Scheme 2. Representative full mass fragmentations of molecular ion mass of **4a**.

3.2. Nanocatalyst characterization

FT-IR spectra of GO (a), GO@dopamine (b), and GO@dopamine-Cu (c) are shown in Figure 1. As can be seen in Figure 1a, the stretching frequencies at 1725 and 1622 cm^{-1} corresponding to carboxylic acid's carbonyl groups and C=C bond of phenyl rings in GO. The bands at 1050 and 1230 cm^{-1} are of C-O stretching frequencies of hydroxyl and epoxy groups on the GO surface, respectively. In Figure

1b, the bands at 1358 and 1045 cm^{-1} stretching frequencies correspond to the C-O and C-N bonds, respectively, in which dopamine interacted with GO functional groups. Figure 1c shows the spectrum of GO@dopamine-Cu in which nearly all peaks of GO and dopamine are shown. The decrease of the peak at 3350 cm^{-1} is attributed to the immobilization of Cu on dopamine and GO surfaces.

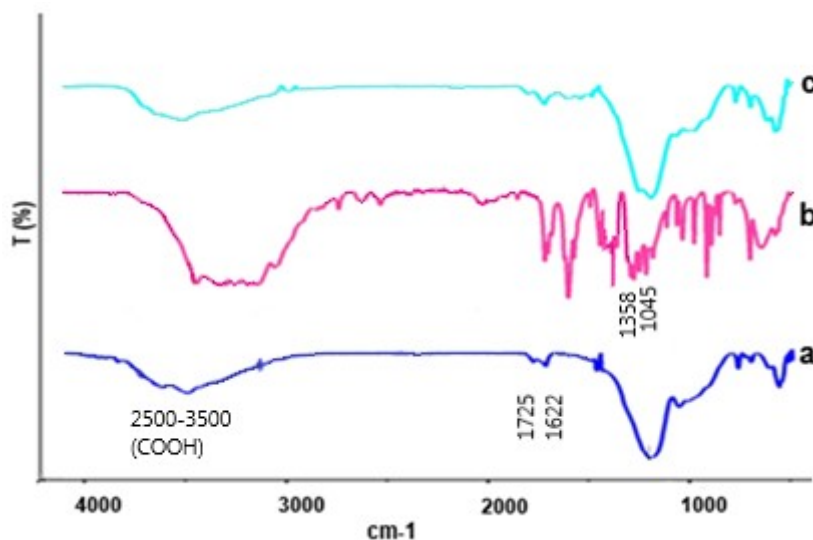


Figure 1. FT-IR spectra of GO (a), GO@dopamine (b), and GO@dopamine-Cu (c).

The XRD patterns of GO and GO@dopamine-Cu are shown in Figure 2. Peaks at 2θ 25° and 43° correspond to GO crystalline sheets.

Peaks at 2θ 9.7° , 23.9° , 36.5° , and 42.1° are corresponding to functionalized GO by dopamine and Cu immobilization.

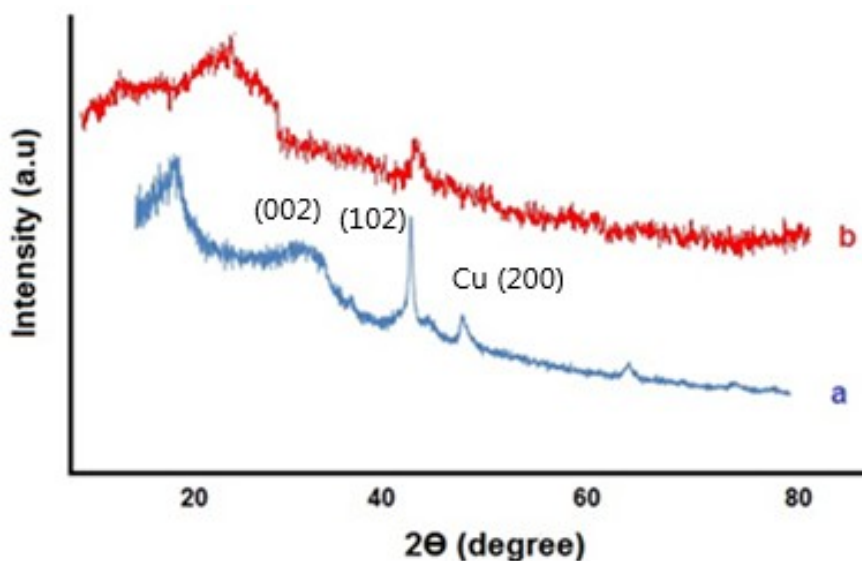


Figure 2. XRD patterns of GO@dopamine-Cu (a) and GO (b).

The morphology of GO@dopamine-Cu according to the scanning electron microscopy (SEM) reveals that the GO parent morphology is retained, as shown in Figure 3a. Transmittance electron microscopy (TEM) image of nanocatalyst obviously showed the graphene oxide nanosheets link to dopamines and also immobilized copper nanoparticles (Cu-NPs) on the

GO nanosheets are shown in Figure 3b. These observations confirmed the immobilization of Cu-NPs on the surface of GO@dopamine nanosheets. EDS data demonstrated that the related elements (C, Cu, O, and N) of GO@dopamine-Cu displayed 53.8, 24.6, 11.4, and 10.2 %, respectively (Figure 3c).

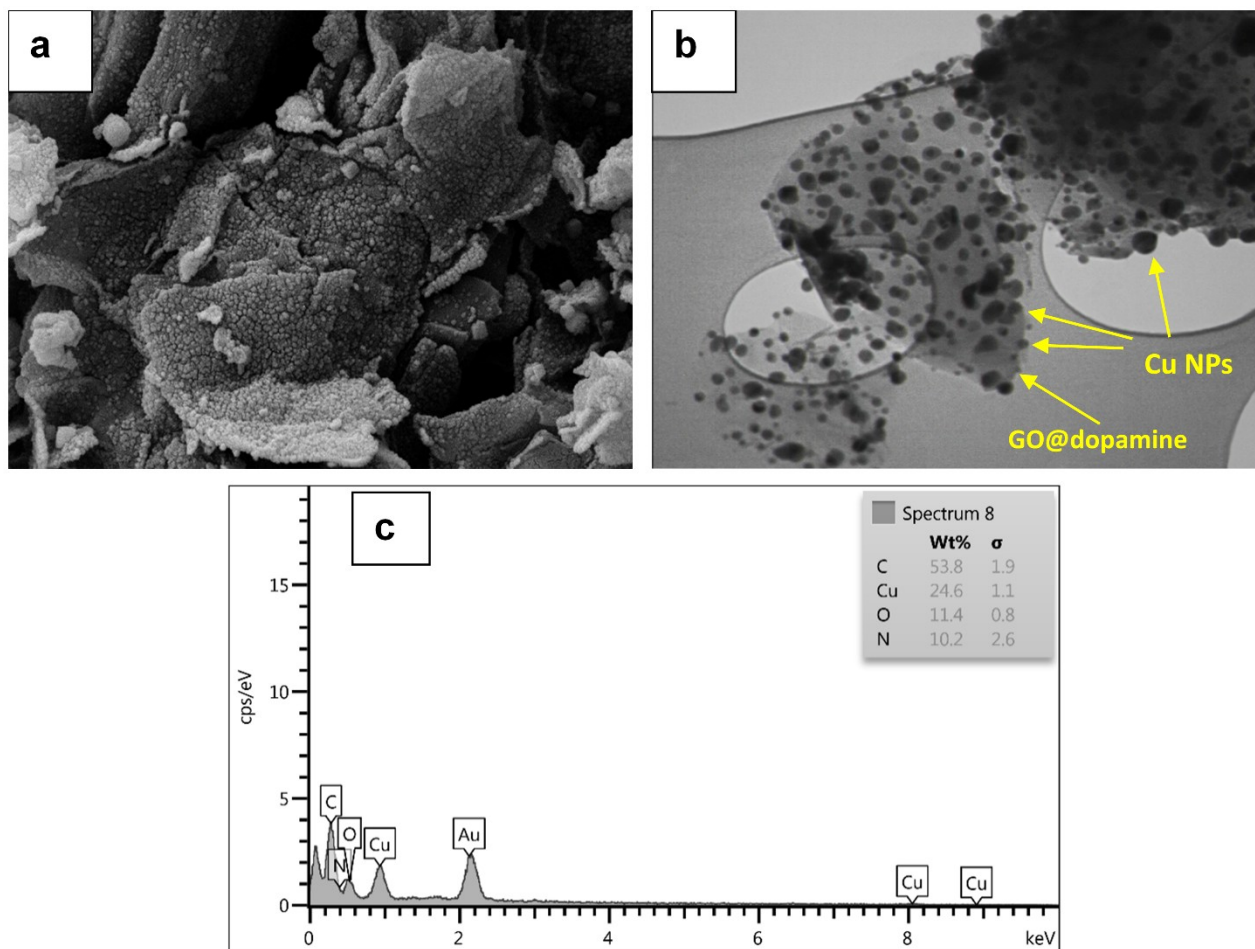


Figure 3. SEM (a) and TEM images (b) and EDS data of GO@dopamine-Cu (c).

TGA and DTA of GO@dopamine-Cu are shown in Figure 4. The weight loss at the range of 0-100 °C corresponds to the loss of solvents and at the range of 135-200 °C related to the loss of copper ions from the nanocatalyst surface. The weight loss at

the 200-400 °C range was attributed to the loss of dopamine ligands. Finally, the weight loss at up to 400 °C corresponded to the decomposition of the GO structure.

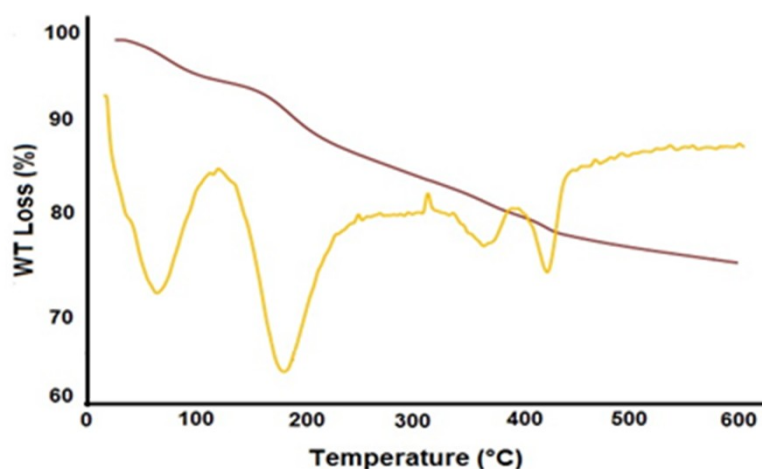


Figure 4. TGA-DTA analysis of GO@dopamine-Cu.

3.3. Catalytic activity

In this step, the activity of the proposed nanostructure was investigated as a beneficial and eco-friendly component in the synthesis of **4a** as a model reaction. To obtain the optimum situation, different amounts of catalyst, various types of solvents, time, and temperatures were appraised. As evident, the reaction yield is 15% in solvent-free conditions in the presence of 0.05 g of nanocatalyst (Table 2, entry 1). With this amount of nanocatalyst in H₂O:EtOH (1:1/ v:v), the reaction yield slightly increased over a long time (Table 2, entry 2). By increasing the amount of nanocatalyst to 0.06 and 0.10 g in EtOH solvent, no significant change in

reaction progress was observed (86 and 85%, respectively) under the same condition (Table 2, entries 5 and 7). By appraising various solvents (H₂O, CH₃CN, and EtOH) within the optimal state, EtOH had the highest efficiency compared to other solvents, and 0.05 g of nanocatalyst was the best amount of catalyst (Table 2, entry 4). The reaction yield was trace when GO was used solely (Table 2, entry 8). Immobilization of dopamine on GO (in the absence of Cu) slightly increased the reaction yield (12%) on GO@dopamine (Table 2, entry 9). All reaction conditions are outlined in Table 2.

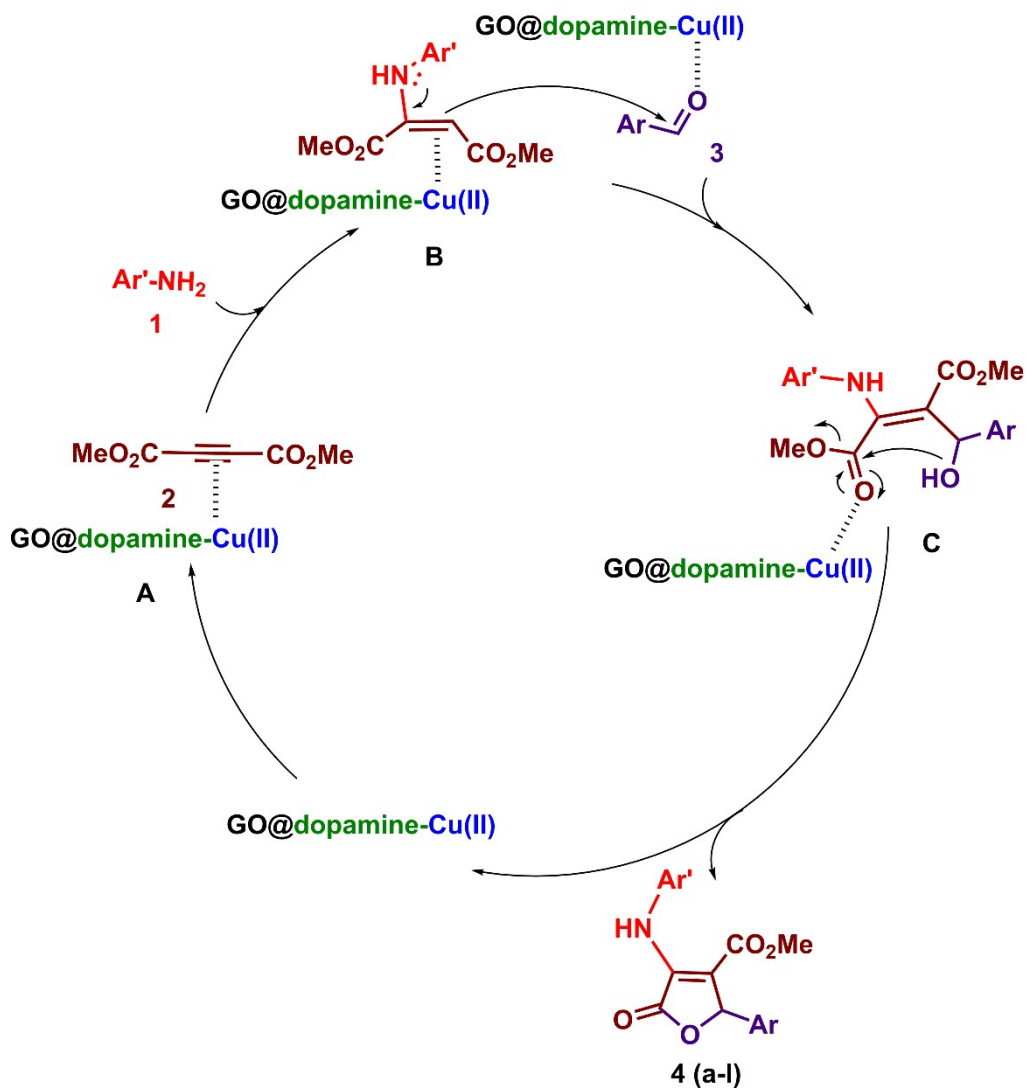
Table 2. Optimization of parameters for the synthesis **4a** as a model reaction.

Entry	solvent	Nanocatalyst amount (g)	Temperature (°C)	Time (min)	Yield (%)
1	-	0.05	110	720	15
2	H ₂ O/EtOH (1:1/ v:v)	0.05	100	1440	20
3	CH ₃ CN	0.05	Reflux	720	40
4	EtOH	0.05	Reflux	65	82
5	EtOH	0.06	Reflux	65	86
6	EtOH	0.025	Reflux	65	45
7	EtOH	0.10	Reflux	65	85
8	EtOH	0.06 (GO)	Reflux	720	trace
9	EtOH	0.06 (GO@dopamine)	Reflux	720	12

The plausible mechanism for the synthesis of **4** was presented in Scheme 3. First, the nanocatalyst coordinated to dimethyl acetylenedicarboxylate (**2**), produced intermediate (**A**), then nucleophilic attacking of primary aromatic amine (**1**) to polarized acetylenic carbon atom formed intermediate (**B**) as an enamine. Afterward, the nucleophilic attack of enamine **B** to the polarized carbonyl group of an aldehyde (**3**) formed intermediate (**C**). The cyclization of this intermediate via an intramolecular attack of the hydroxyl group on the activated esteric carbonyl group formed the desired heterocyclic compounds **4** (Scheme 3).

3.4. Recyclability of nanocatalyst

To evaluate the recyclability of the GO@dopamine-Cu nanocatalyst, the reusability of this nanocatalyst was examined in the one-pot reaction of aniline **1a**; dimethyl acetylenedicarboxylate **2** and benzaldehydes **3a** for the synthesis of **4a** as a model reaction based on optimum conditions (Figure 5). The nanocatalyst was separated at the end of each reaction by centrifugation and then dried by elution with ethanol. Then, the nanocatalyst is used for the next run, indicating that the proposed nanocatalyst is recycled in five runs. After five runs, the recycled nanocatalyst showed no significant decrease in catalytic activity (Figure 5).



Scheme 3: Plausible reaction mechanism for the synthesis of **4** in the presence of GO@dopamine-Cu nanocatalyst.

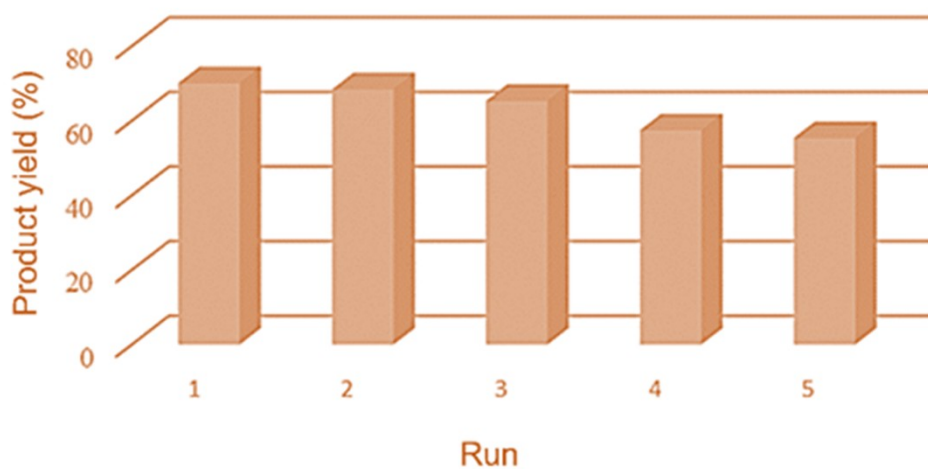


Figure 5: Recyclability of GO@dopamine-Cu in the preparation of **4**.

4. CONCLUSION

In summary, in this work, GO@dopamine-Cu nanocatalyst was synthesized and characterized its structure by FT-IR, XRD, SEM, TEM, EDX, and TGA-DTA techniques. This nanocatalyst was used for a one-pot, three-component reaction of an aromatic aldehyde, arylamine, and acetylenic carboxylate for the synthesis of full substituted furan-2(5H)-ones derivatives in high yield. All of the heterocyclic structures were characterized and confirmed their structures by spectroscopic methods. We concluded that GO@dopamine-Cu is an efficient nanocatalyst for the one-pot synthesis of full substituted furan-2(5H)-one derivatives. The main advantages of this work were easy reaction, high performance, and easy catalyst recyclability. This nanocatalyst recovered at least five times with negligible decreasing catalytic activity.

5. CONFLICT OF INTEREST

The authors declare no conflict of interest.

6. ACKNOWLEDGMENTS

We would like to thank the Research Council of Urmia University for supporting this work.

7. REFERENCES

- Subodh S, Prakash K, Masram DT. A reversible chromogenic covalent organic polymer for gas sensing applications. *Dalton Transactions*. 2020;49(4):1007–10. Available from: [<URL>](#).
- Yadav D, Awasthi SK. An unsymmetrical covalent organic polymer for catalytic amide synthesis. *Dalton Transactions*. 2020;49(1):179–86. Available from: [<URL>](#).
- Subodh, Prakash K, Masram DT. Chromogenic covalent organic polymer-based microspheres as solid-state gas sensor. *Journal of Material Chemistry C*. 2020;8(27):9201–4. Available from: [<URL>](#).
- Presolski S, Pumera M. Graphene Oxide: Carbocatalyst or Reagent? *Angewandte Chemie, International Edition*. 2018 Dec 17;57(51):16713–5. Available from: [<URL>](#).
- Zhang M, Liu YH, Shang ZR, Hu HC, Zhang ZH. Supported molybdenum on graphene oxide/Fe₃O₄: An efficient, magnetically separable catalyst for one-pot construction of spiro-oxindole dihydropyridines in deep eutectic solvent under microwave irradiation. *Catalysis Communications*. 2017 Jan;88:39–44. Available from: [<URL>](#).
- Subodh, Mogha NK, Chaudhary K, Kumar G, Masram DT. Fur-Imine-Functionalized Graphene Oxide-Immobilized Copper Oxide Nanoparticle Catalyst for the Synthesis of Xanthene Derivatives. *ACS Omega*. 2018 Nov 30;3(11):16377–85. Available from: [<URL>](#).
- Yadav D, Awasthi SK. A Pd NP-confined novel covalent organic polymer for catalytic applications. *New Journal of Chemistry*. 2020;44(4):1320–5. Available from: [<URL>](#).
- Yadav D, Awasthi SK. A Pd confined hierarchically conjugated covalent organic polymer for hydrogenation of nitroaromatics: catalysis, kinetics, thermodynamics and mechanism. *Green Chemistry*. 2020;22(13):4295–303. Available from: [<URL>](#).
- Subodh, Prakash K, Masram DT. Silver Nanoparticles Immobilized Covalent Organic Microspheres for Hydrogenation of Nitroaromatics with Intriguing Catalytic Activity. *ACS Applied Polymer Materials*. 2021 Jan 8;3(1):310–8. Available from: [<URL>](#).
- Chaudhary K, Subodh, Prakash K, Mogha NK, Masram DT. Fruit waste (Pulp) decorated CuO NFs as promising platform for enhanced catalytic response and its peroxidase mimics evaluation. *Arabian Journal of Chemistry*. 2020 Apr;13(4):4869–81. Available from: [<URL>](#).
- Stankovich S, Dikin DA, Piner RD, Kohlhaas KA, Kleinhammes A, Jia Y, et al. Synthesis of graphene-based nanosheets via chemical reduction of exfoliated graphite oxide. *Carbon*. 2007 Jun;45(7):1558–65. Available from: [<URL>](#).
- Dreyer DR, Todd AD, Bielawski CW. Harnessing the chemistry of graphene oxide. *Chemical Society Reviews*. 2014 Jul 7;43(15):5288–301. Available from: [<URL>](#).
- Compton OC, Nguyen ST. Graphene Oxide, Highly Reduced Graphene Oxide, and Graphene: Versatile Building Blocks for Carbon-Based Materials. *Small*. 2010 Mar 22;6(6):711–23. Available from: [<URL>](#).
- Noori S, Ghorbani-Vaghei R, Azadbakht R, Karamshahi Z, Koolivand M. Graphene-oxide/schiff base N2O4 ligand-palladium: A new catalyst for the synthesis of furan derivatives. *Journal of Molecular Structure*. 2022 Feb;1250:131849. Available from: [<URL>](#).
- Dömling A. Recent Developments in Isocyanide Based Multicomponent Reactions in Applied Chemistry. *Chemical Reviews*. 2006 Jan 1;106(1):17–89. Available from: [<URL>](#).
- Pour M, Špulák M, Buchta V, Kubanová P, Vopršalová M, Wsól V, et al. 3-Phenyl-5-acyloxymethyl-2 H , 5H -furan-2-ones: Synthesis and Biological Activity of a Novel Group of Potential Antifungal Drugs. *Journal of Medicinal Chemistry*. 2001 Aug 1;44(17):2701–6. Available from: [<URL>](#).
- Wu J, Cheng Y, Zhao X, Liu X, Sun W, Ren H, et al. Antibacterial activity and biological performance of a novel antibacterial coating containing a halogenated furanone compound loaded poly(L-lactic acid) nanoparticles on microarc-oxidized titanium. *International Journal of Nanomedicine*. 2015 Jan;727. Available from: [<URL>](#).
- Tejedor D, García-Tellado F. Chemo-differentiating ABB ' multicomponent reactions. Privileged building blocks. *Chemical Society Reviews*. 2007;36(3):484–91. Available from: [<URL>](#).
- Shirzaei M, Mollashahi E, Taher Maghsoodlou M, Lashkari M. Novel synthesis of silica-coated magnetic nano-particles based on acidic ionic liquid, as a highly efficient catalyst for three component system leads to

furans derivatives. Journal of the Saudi Chemical Society. 2020 Feb;24(2):216–22. Available from: [<URL>](#).

20. Weber V. Novel 4,5-Diaryl-3-hydroxy-2(5H)-furanones as Anti-Oxidants and Anti-Inflammatory Agents. Bioorganic & Medicinal Chemistry. 2002 Jun;10(6):1647–58. Available from: [<URL>](#).

21. Lattmann E, Ayuko WO, Kinchinaton D, Langley CA, Singh H, Karimi L, et al. Synthesis and evaluation of 5-arylated 2(5H)-furanones and 2-arylated pyridazin-3(2H)-ones as anti-cancer agents. Journal of Pharmacy and Pharmacology. 2010 Feb 18;55(9):1259–65. Available from: [<URL>](#).

22. El-Tombary AA, Abdel-Ghany YS, Belal ASF, Shams El-Dine SA, Soliman FSG. Synthesis of some substituted furan-2(5H)-ones and derived quinoxalinones as potential anti-microbial and anti-cancer agents. Medicinal Chemistry Research. 2011 Sep;20(7):865–76. Available from: [<URL>](#).

23. Lipshutz BH. Five-membered heteroaromatic rings as intermediates in organic synthesis. Chemical Reviews. 1986;86(5):795–819.

24. Mortensen DS, Rodriguez AL, Carlson KE, Sun J, Katzenellenbogen BS, Katzenellenbogen JA. Synthesis and Biological Evaluation of a Novel Series of Furans: Ligands Selective for Estrogen Receptor α . Journal of Medicinal Chemistry. 2001 Nov 1;44(23):3838–48. Available from: [<URL>](#).

25. Bassetti M, D'Annibale A, Fanfoni A, Minissi F. Synthesis of α,β -Unsaturated 4,5-Disubstituted γ -Lactones via Ring-Closing Metathesis Catalyzed by the First-Generation Grubbs' Catalyst. Organic Letters. 2005 Apr 1;7(9):1805–8. Available from: [<URL>](#).

26. Bock I, Bornowski H, Ranft A, Theis H. New aspects in the synthesis of mono- and dialkylfurans. Tetrahedron. 1990 Jan;46(4):1199–210. Available from: [<URL>](#).

27. Takahashi S, Kubota A, Nakata T. Total synthesis of muconin. Tetrahedron Letters. 2002 Nov;43(48):8661–4. Available from: [<URL>](#).

28. Bandurraga MM, Fenical W, Donovan SF, Clardy J. Pseudopterolide, an irregular diterpenoid with unusual cytotoxic properties from the Caribbean sea whip Pseudopterogorgia acerosa (Pallas)(Gorgonacea). Journal of the American Chemical Society. 1982;104(23):6463–5.

29. Padakanti S, Pal M, Yeleswarapu KR. An improved and practical synthesis of 5,5-dimethyl-3-(2-propoxy)-4-(4-methanesulfonylphenyl)-2-(5H)-furanone (DFP—a selective inhibitor of cyclooxygenase-2). Tetrahedron. 2003 Sep;59(40):7915–20. Available from: [<URL>](#).

30. Lee ES, Park BC, Paek SH, Lee YS, Basnet A, Jin DQ, et al. Potent Analgesic and Anti-inflammatory Activities of 1-Furan-2-yl-3-pyridin-2-yl-propenone with Gastric Ulcer Sparing Effect. Biological & Pharmaceutical Bulletin. 2006;29(2):361–4. Available from: [<URL>](#).

31. Rossi R, Bellina F, Biagetti M, Mannina L. Stereocontrolled synthesis of lissoclinolide by sequential transition metal-catalyzed lactonization/cross-coupling reactions. Tetrahedron Letters. 1998 Oct;39(42):7799–802. Available from: [<URL>](#).

32. Levy L. 5H-Furan-2-ones from fungal cultures of *Aporpium caryae*. Phytochemistry. 2003 Jan;62(2):239–43. Available from: [<URL>](#).

33. Hofnung M, Quillardet P, Michel V, Touati E. Genotoxicity of 2-nitro-7-methoxy-naphtho[2,1-b]furan (R7000): A case study with some considerations on nitrofurantoin and nifuroxazide. Research in Microbiology. 2002 Sep;153(7):427–34. Available from: [<URL>](#).

34. Wahab Khan M, Jahangir Alam M, Rashid MA, Chowdhury R. A new structural alternative in benzo[b]furans for antimicrobial activity. Bioorganic & Medicinal Chemistry. 2005 Aug;13(16):4796–805. Available from: [<URL>](#).

35. Pour M, Špulák M, Balšánek V, Kuneš J, Kubanová P, Buchta V. Synthesis and structure-antifungal activity Relationships of 3-Aryl-5-alkyl-2,5-dihydrofuran-2-ones and Their Carbanalogues: further refinement of tentative pharmacophore group. Bioorganic & Medicinal Chemistry. 2003 Jul;11(13):2843–66. Available from: [<URL>](#).

36. Shafiee MRM, Mansoor SS, Ghashang M, Fazlinia A. Preparation of 3,4,5-substituted furan-2(5H)-ones using aluminum hydrogen sulfate as an efficient catalyst. Comptes Rendus Chimie. 2014 Feb;17(2):131–4. Available from: [<URL>](#).

37. Karamshahi Z, Ghorbani-Vaghei R. Efficient synthesis of multiply substituted furans using BF₃·Propyl/dopamine/Pd as a green catalyst. Applied Organometallic Chemistry. 2020 Apr;34(4):e5530. Available from: [<URL>](#).

38. Wipf P, Rahman LT, Rector SR. A General Strategy for Five-Membered Heterocycle Synthesis by Cycloelimination of Alkynyl Ketones, Amides, and Thioamides. The Journal of Organic Chemistry. 1998;63(21):7132–3.

39. Golonka AN, Schindler CS. Iron(III) chloride-catalyzed synthesis of 3-carboxy-2,5-disubstituted furans from γ -alkynyl aryl- and alkylketones. Tetrahedron. 2017 Jul;73(29):4109–14. Available from: [<URL>](#).

40. Kangani M, Hazeri N, Maghsoodlou MT. Synthesis of pyrrole and furan derivatives in the presence of lactic acid as a catalyst. Journal of the Saudi Chemical Society. 2017 Feb;21(2):160–4. Available from: [<URL>](#).

